A&A 470, 173–178 (2007)
DOI: 10.1051/0004-6361:20077151

Astronomy & Astrophysics

The formation of S0 galaxies: evidence from globular clusters

J. M. Barr[1], A. G. Bedregal[1], A. Aragón-Salamanca[1], M. R. Merrifield[1], and S. P. Bamford[1,2]

[1] The School of Physics & Astronomy, University of Nottingham, University Park, Nottingham, NG7 2RD, UK
e-mail: jordi.barr@nottingham.ac.uk
[2] Institute of Cosmology and Gravitation, Mercantile House, Hampshire Terrace, University of Portsmouth, Portsmouth, PO1 2EG, UK

Received 23 January 2007 / Accepted 26 April 2007

ABSTRACT

Aims. We devise a simple experiment to test the theory that lenticular (S0) galaxies form from spirals whose star formation has been shut down. An individual galaxy's fading is measured using the globular cluster specific frequency (S_N), defined as the number of globular clusters normalised by the galaxy luminosity. This is compared with a spectroscopically-derived age estimate.
Methods. We make NTT/EMMI long-slit spectroscopic observations of 11 S0 galaxies at $z < 0.006$. We measure the absorption-line indices, Hδ, Hγ, Mgb, Fe5270 and Fe5335 within the central $r_e/8$. By inverting single-stellar population models, luminosity-weighted mean ages, metallicities and α-element abundance ratios are derived. We estimate the amount of fading a galaxy has undergone by comparing each galaxy's S_N with its deviation from the mean spiral S_N.
Results. Galaxies with higher S_N have older stellar populations. Moreover, we find that the zero-point and amount of fading is consistent with a scenario where lenticulars are formed by the quenching of star formation in spiral galaxies. Our data also rule out any formation method for S0s which creates a large number of new globular clusters. We confirm that previous results showing a relationship between S_N and color are driven by the S_N–Age relation. Five galaxies show detectable Hβ, [O III], Hα or [N II] emission lines. However, only in the two youngest galaxies is this emission unambiguously from star formation.
Conclusions. Our results are consistent with the theory that S0 galaxies are formed when gas in normal spirals is removed, possibly as a result of a change in environment. The on-going star formation in the youngest galaxies hints that the timescale of quenching is $\lesssim$1 Gyr. We speculate, therefore, that the truncation of star formation is a rather gentle process unlikely to involve a rapid burst of star formation.

Key words. galaxies: formation – galaxies: evolution – galaxies: structure – galaxies: star clusters

1. Introduction

Lenticular (S0) galaxies live at the intersection of spirals and ellipticals on Hubble's Tuning Fork. As a class, they provide a useful exemplar of what could be an intermediate stage of a galaxy's evolution. They also give us insight into galaxy formation and its relationship with environment. Hubble Space Telescope observations of distant galaxy clusters show that the proportion of S0s declines with redshift, while the abundance of spirals increases (Dressler et al. 1997). The idea that star formation in spiral galaxies is cut off when they enter a denser environment therefore seems a plausible one. The mechanism by which this cessation is achieved is a topic of active debate and many scenarios have been proposed. These include close encounters or mergers, which increase the luminosity of the bulge component by heating the central parts of the disk or triggering a central star-formation episode (e.g. Mihos & Hernquist 1994; Bekki 1998). Galaxy harassment, where a galaxy undergoes many close but fleeting high-speed interactions with other galaxies (e.g. Moore et al. 1996, 1998) is predicted to have a similar effect. Other scenarios involve the interaction of a spiral galaxy with the intracluster gas either by by ram-pressure stripping (e.g. Gunn & Gott 1972; Quilis et al. 2000; Vollmer et al. 2001; Sun et al. 2006), or over a longer period, for example by removal of gas from the galaxy halo (e.g. Larson et al. 1980), or by heating of gas within the galaxy by the ICM – so-called thermal evaporation (Cowie & Songaila 1977). See Bosselli & Gavazzi (2006) for a thorough discussion of the various mechanisms.

These transformation scenarios can be separated in a number of ways, perhaps contrasting the effects of other galaxies against intracluster gas, or looking at gravitational versus hydrodynamical drivers. However, from an observational point of view the most accessible information is how rapid or violent a particular transformation is. Even if S0 galaxies are formed via a unique mechanism, post hoc observations will not easily distinguish between those transformations which yield a similar final state. As well as looking for consistency with a fading scenario, this study will test whether lenticular formation is more likely to be due to a violent or a passive episode.

Direct observational studies of S0 formation, as opposed to simulations, are rather thin on the ground. Dressler et al. (2004) show evidence from composite spectra in rich clusters that S0 galaxies probably experienced a recent burst of star formation. It has also been suggested that the mechanism of truncation was more violent at higher redshift (see Boselli et al. 2006).

Circumstantial evidence in support of quiet lenticular formation comes from observations of the S0 Tully-Fisher relation (Bedregal et al. 2006). In the B-band this is, on average, ~1.3 mag fainter than the spiral relation of Sakai et al. (2000). The scatter is also much larger. This can be interpreted as a fading of a stellar population of a given rotational velocity, where the fading begins over a range of epoch, corresponding to the cessation of a galaxy's star formation. This does, however, presume that the rotational velocity of galaxy is not greatly altered in a transformation from spiral to S0. And indeed that you can

accurately disentangle the rotational velocity from velocity dispersion in an S0 using the combination as a proxy for mass. This result also relies on the fact that the progenitors of the current generation of S0s can be compared directly with local spirals. Were there to be strong evolution in the masses of spiral galaxies since $z \sim 0.5$ this comparison would not be valid. There is little consensus at present on whether this is the case; see Flores et al. (2006) and Weiner et al. (2006) for contrasting viewpoints.

A simple observational test between formation mechanisms is provided by globular clusters. It is widely presumed that globular clusters are created and disrupted during the kind of violent galaxy interaction like a merger (e.g. Ashman & Zepf 1998). In contrast, if we assume that a quieter scenario (e.g. ram-pressure stripping, thermal evaporation) will roughly preserve the number, and luminosity, of a galaxy's globular clusters, we can use the specific frequency of globular clusters (S_N) as a diagnostic tool. Specific frequency is defined as the number of globular clusters per unit luminosity in a galaxy. If star formation shuts down in a spiral galaxy, S_N will increase as the galaxy fades. This quantity can therefore be used to trace the time since the last star formation episode. If the passive mechanism holds, then we expect to see a correlation between stellar age and S_N in S0s. No such correlation is expected in mergers and close gravitational encounters as these are not expected to preserve S_N.

Aragón-Salamanca et al. (2006) examined color as a function of S_N for a sample of 12 S0 galaxies. They used color as a proxy for age and found that U, B, V, R, I colors are related to S_N in the manner expected of a fading stellar population. That is to say the redder galaxies have higher S_N, i.e. have undergone more fading. Moreover, the distribution of colors and S_N is entirely consistent with models predicting the color and luminosity evolution of single-stellar populations (e.g. Worthey 1994; Bruzual & Charlot 2003). Furthermore, comparing values of S_N with spirals indicated that S0s had faded by a factor of ∼3, the same amount found by Bedregal et al. (2006) for the S0 Tully-Fisher relation.

The problem that observations of color and luminosity encounter is the age-metallicity degeneracy. It has not been possible to say for certain that the physical effect driving the color-S_N relation is age. Clearly, what is needed is a test that can separate age and metallicity, and ideally mass and luminosity as well. In this paper we use spectroscopic observations of absorption-line strengths to derive physical attributes of a sample of S0s and compare these with S_N. Section 2 describes the observations and data reduction. Section 3 gives results. We work towards putting our galaxies on the Age−S_N plot in Sect. 4. Conclusions are presented in Sect. 5. Throughout we use $H_0 = 70\,\mathrm{km\,s^{-1}\,Mpc^{-1}}$, $\Omega_\mathrm{m} = 0.3$, $\Omega_\Lambda = 0.7$.

2. Observations and data reduction

2.1. Sample selection

The 11 lenticular galaxies in our sample are a subset of those with globular cluster observations in Kundu & Whitmore (2001b). The galaxies are chosen to cover a range in luminosity and globular cluster specific frequency. All apart from two (NGC 3056 and NGC 3115B) reside in group or poor cluster environments. See Kundu & Whitmore (2001b) for more details.

2.2. Globular cluster specific frequency

The specific frequency of globular clusters is defined as,

$$S_N = N_\mathrm{t} 10^{0.4(M_V+15)}$$

where N_t is the total number of clusters and M_V is the total V-band magnitude of the galaxy[1].

HST-derived values of local S_N for S0s come from Kundu & Whitmore (2001b). Local in this case refers to the fact that the WFPC2 field-of-view only covers the central part of the galaxy and so the number of clusters and normalising luminosity are not those of the galaxy as a whole. The ratio of local to global S_N depends to some extent on luminosity, though the uncertainties are high. See Kundu & Whitmore (2001a,b) for more details. We use the directly-derived, local values of S_N. There is also a closer correspondence of scales between these values and our spectral aperture. We note that the average local values of S_N for spirals is 0.4 (Goudfrooij et al. 2003), lenticulars 1.0 (Kundu & Whitmore 2001b), and ellipticals 2.4 (Kundu & Whitmore 2001a).

Table 1. Instrument parameters.

Telescope	NTT
Instrument	EMMI
Wavelength range	3500−7200 Å
Grism	LR5
Slit width	1.″02
Spatial resolution	0.″33 pix^{-1}
Spectral resolution*	119 km s^{-1}

* Median instrumental resolution at 5500 Å.

Table 2. Targets and exposure times.

Galaxy	T (s)	M_V	S_N	r_e (″)	z
NGC 1201	3600	−20.8	1.1 ± 0.5	28.00	0.005722
NGC 1332	2700	−21.2	2.2 ± 2.7	28.00	0.005219
NGC 1389	3600	−19.5	0.5 ± 0.4	15.04	0.003342
NGC 1400	4500	−20.6	2.9 ± 1.1	29.32	0.001964
NGC 1553	2700	−21.5	0.5 ± 0.1	65.63	0.004227
NGC 1581	7200	−18.2	0.2 ± 0.9	10.64	0.005390
IC 1919	19800	−18.2	1.1 ± 1.7	60.00	0.004511
NGC 2902	2700	−20.2	0.3 ± 0.4	15.39	0.006611
NGC 3056	2700	−18.9	0.6 ± 0.7	50.95	0.003229
NGC 3115B	14400	−17.9	6.8 ± 2.4	16.87	0.002316
NGC 3156	3600	−18.9	0.4 ± 0.4	14.36	0.004396

M_V and S_N from Kundu & Whitmore (2001b). Half light radius from RC3 catalogue (Corwin et al. 1994) except IC1919 where r_e estimated from light profile in slit.

2.3. EMMI data

Spectroscopic observations of our targets was obtained on the NTT at La Silla during 2005 December 1–3. Observations were made using EMMI (Dekker et al. 1986) in its long-slit, low-resolution grism spectroscopy mode (RILD). Seeing varied from 0.″45 to 1.″4 FWHM. Instrumental parameters are given in Table 1. Properties of the targets are detailed in Table 2.

Data is reduced in standard fashion. The spectra are bias-subtracted and flat-fielded using lamp flats. Wavelength calibration is performed using arc spectra from the same night. We check the accuracy of the solution using transformed arc spectra. The offset between measured vs. actual wavelength for a line increases linearly with distance from the blaze wavelength

[1] Note that we fix the error in Ashman & Zepf (1998) where S_N is defined with a negative power. See Harris & van den Bergh (1981).

Table 3. Derived spectroscopic parameters.

Galaxy	σ (km s^{-1})	Hγ (Å)	Hδ (Å)	Mgb (Å)	$\langle$Fe$\rangle$ (Å)	log Age (log Gyr)	[Fe/H]	[α/Fe]
NGC1201	111 ± 3	-7.26 ± 0.04	-2.19 ± 0.03	4.70 ± 0.04	3.08 ± 0.03	0.950 ± 0.022	0.360 ± 0.022	0.185 ± 0.012
NGC1332	240 ± 4	-7.02 ± 0.04	-1.76 ± 0.03	5.04 ± 0.04	2.75 ± 0.03	1.103 ± 0.024	0.270 ± 0.023	0.325 ± 0.012
NGC1389	82 ± 2	-6.08 ± 0.05	-1.75 ± 0.04	4.25 ± 0.05	3.12 ± 0.04	0.625 ± 0.044	0.467 ± 0.034	0.125 ± 0.014
NGC1400	215 ± 7	-6.62 ± 0.04	-1.36 ± 0.03	5.05 ± 0.04	2.74 ± 0.03	0.981 ± 0.024	0.345 ± 0.023	0.341 ± 0.011
NGC1553*	137 ± 1	-6.78 ± 0.03	-1.33 ± 0.02	4.33 ± 0.03	2.94 ± 0.03	0.850 ± 0.025	0.305 ± 0.024	0.175 ± 0.011
NGC1581*	74 ± 5	1.11 ± 0.07	4.70 ± 0.05	1.83 ± 0.11	1.73 ± 0.09	0.204 ± 0.025	-0.315 ± 0.005	0.075 ± 0.056
IC1919	76 ± 1	-2.32 ± 0.18	1.30 ± 0.12	2.42 ± 0.30	2.57 ± 0.23	0.371 ± 0.075	0.072 ± 0.175	0.016 ± 0.027
NGC2902*	108 ± 1	-6.66 ± 0.09	-2.12 ± 0.07	4.68 ± 0.11	2.91 ± 0.08	0.985 ± 0.062	0.291 ± 0.058	0.225 ± 0.027
NGC3056*	74 ± 5	-3.90 ± 0.06	0.80 ± 0.04	2.69 ± 0.07	2.36 ± 0.06	0.617 ± 0.051	-0.121 ± 0.041	0.025 ± 0.025
NGC3115B	66 ± 1	-3.81 ± 0.31	0.29 ± 0.22	2.81 ± 0.43	2.03 ± 0.33	0.933 ± 0.180	-0.321 ± 0.166	0.217 ± 0.155
NGC3156*	72 ± 2	3.95 ± 0.05	6.37 ± 0.03	1.72 ± 0.07	1.76 ± 0.06	0.010 ± 0.009	-0.187 ± 0.044	0.036 ± 0.025

Stars denote those galaxies with line emission in Hβ, [O III] [N II], Hα or [S II].

at 5300 Å. This typically reaches a maximum of 0.1 Å at 4000 Å and 7000 Å.

The sky is removed by fitting a 3rd order Legendre polynomial to a 100″ aperture either side of the galaxy. The spectra are extracted from an aperture of width equal to 1/8th of the half-light radius. Flux calibrations are made using observations of spectrophotometric standard White Dwarfs, G158-100, Feige 110, GD50 and GD108 undertaken during the same run.

To derive accurate kinematic information, observations of three (K2III, G0V, F5V) template stars are made. These are reduced in exactly the same way as the science data.

2.4. Kinematics and Absorption-line Indices

Velocity dispersions (σ) are derived using the method of Gebhardt et al. (2000) and checked for consistency with the code made available by Michele Cappellari[2] (see Cappellari & Emsellem 2004). Both methods gave consistent results. Seven galaxies have $\sigma \lesssim$ the instrumental resolution. This means they could be subject to systematic uncertainties. However, velocity dispersions are only used to provide a correction for the line strength measurements to the rest frame. Errors that may be introduced in this way are small; for example, a factor of two overestimate in the value of σ causes errors of ∼3% in the Hβ index and ∼5% in Mgb. These are of the same order as the random errors.

Absorption line indices are derived from the spectra. We use Mgb and $\langle$Fe$\rangle$ (the mean of Fe5270, Fe5335) from the Lick/IDS system as defined in Worthey et al. (1994). In addition we calculate the H$\beta_{\rm G}$ index as in Jørgensen (1997) and the Hγ and Hδ indices of Worthey & Ottaviani (1997). Line indices are corrected for the effect of velocity dispersion following the technique described in Davies et al. (1993). We use the models of Thomas et al (2003, 2004) to assign relative ages, metallicities and α-element abundance ratios ([α/Fe]) from the measured index values. Derived properties for the sample are listed in Table 3.

3. Results

3.1. Balmer lines, Hβ vs. Hγ and Hδ

Traditionally, in trying to quantify age and metallicity using spectroscopy, the Hβ index is used as the primary age indicator together with the Mgb and $\langle$Fe$\rangle$ indices. An alternative, particularly useful at higher redshift is to use a combination of the higher order Balmer lines, Hγ and Hδ. However, it has been noted by various investigators (e.g. Terlevich et al. 1999; Poggianti et al. 2001; Kuntschner et al. 2002) that Hβ tends to give systematically older ages than Hγ + Hδ.

There are two complementary but quite different effects responsible for this discrepancy. Firstly, Hγ and Hδ are more sensitive to the effects of enhanced [α/Fe]. Derivations of ages for early type galaxies using these indices which do not account for [α/Fe] lead to younger ages than through Hβ (see Thomas et al. 2004). Secondly, unresolved emission can "fill in" the stellar absorption line, causing it to appear weaker than it otherwise would. In galaxies with relatively little on-going star formation, this effects the lower-excitation states more than the higher. This means that young galaxies could appear artificially old when using Hβ as the age diagnostic rather than the higher-order Balmer lines.

We correct for the first phenomenon using models which include variable [α/Fe]. To gauge the effect of unresolved emission, we note that, of our sample, 2 galaxies have ostensible emission in Hβ. Three more have [O III], Hα or [N II]. Moreover, if we plot the Balmer lines against one another we find a strong correlation between Hγ and Hδ but only a weak one between Hβ and either Hγ or Hδ. For these reasons, we conclude that Hβ is affected by unresolved emission in several cases. We therefore use the Hγ + Hδ index as the primary age indicator in our analysis.

3.2. Separating age, metallicity, and [α/Fe]

In Fig. 1 we plot $(\mathrm{H}\delta_A + \mathrm{H}\gamma_A)'$ against the combination of indices [MgFe]′ of Thomas et al. (2003)[3]. This quantity, when plotted against Hβ, is designed to be independent of [α/Fe]. However, when plotted against the higher-order Balmer lines, the lack of correspondence in the age-metallicity grids shows that some degeneracy remains. For this reason we are not able to assign unique ages from this figure alone, though our sample does clearly have a range of luminosity-weighted mean ages and metallicities. It is therefore instructive to plot Mgb vs. $\langle$Fe$\rangle$ in Fig. 2. This can be thought of as orthogonal to Fig. 1. We can see immediately that over half the sample have super-solar [α/Fe]. Values of [α/Fe] for galaxy cluster elliptical galaxies typically range over 0–0.25 (Thomas et al. 2005).

We now invert the models to assign meaningful physical quantities to the galaxies. For each galaxy we fit $\mathrm{H}\delta_A$ + $\mathrm{H}\gamma_A$,

[2] http://www.strw.leidenuniv.nl/~mcappell/idl/

[3] $(\mathrm{H}\delta_A + \mathrm{H}\gamma_A)' = -2.5 \log[1 - (\mathrm{H}\delta_A + \mathrm{H}\gamma_A)/82.5]$; [MgFe]′ = (Mg$b$ · [0.72 · Fe5270 + 0.28 · Fe5335])$^{0.5}$.

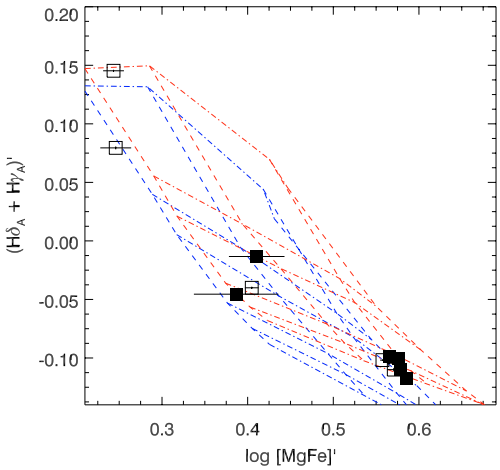

Fig. 1. The higher order Balmer lines versus the Thomas et al. [MgFe]′ index. Open points are those galaxies with either Hα, [O III] or Hβ emission. Grids show the Age-metallicity relations for [α/Fe] = 0.0 (lower) and [α/Fe] = 0.3 (upper). Dashed lines are (left to right) [Fe/H] = –0.3, 0.0, 0.3, 0.5. Dot-dashed lines are ages of (top to bottom) 1, 2, 4, 8, 11, 12 Gyr.

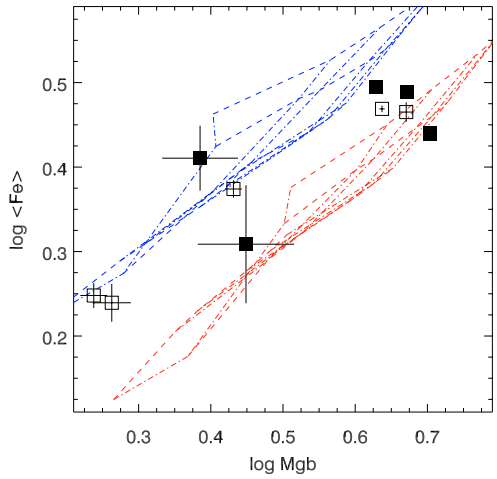

Fig. 2. The Mgb index versus ⟨Fe⟩. Points and grids are equivalent to those in Fig. 1, [α/Fe] = 0.0 (upper), [α/Fe] = 0.3 (lower).

Mgb, and ⟨Fe⟩ simultaneously and linearly interpolate between points on the model grid. The values of age, metallicity and [α/Fe] that minimise χ^2 are adopted. Errors are estimated using a Monte-Carlo method. Each combination of Hδ_A + Hγ_A, Mgb, and ⟨Fe⟩ is perturbed with a Gaussian probability of $\sigma_{\rm index}$ 1000 times assuming that measurements of the indices are independent. Errors in ages, [Fe/H] and [α/Fe] are quoted as the 68th percentile of the distribution.

Errors in age and metallicity are not independent. In theory this means that error bars in age and metallicity are not orthogonal and the effect of either needs to be considered whenever plotting the other. This could also lead to a false (negative) correlation in the age-metallicity relation. In our sample, however, this must be a small effect as log Age vs. [Fe/H] is positively correlated (metallicity is generally lower for younger galaxies). The typical error locus is ≈1/20 of the dynamic range. This indicates that the co-dependence of these errors does not significantly distort the derived physical properties of our sample. We find that the errors in age and metallicity are independent of those of [α/Fe].

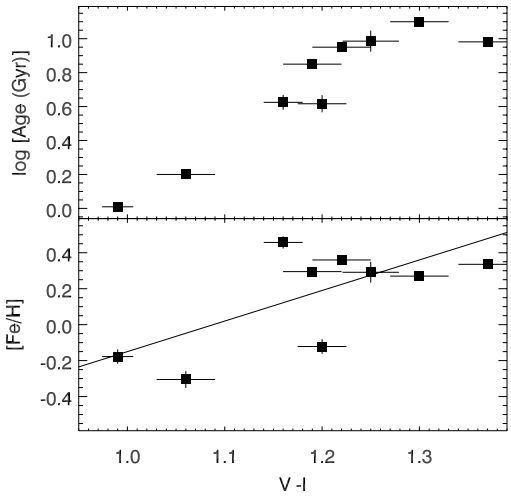

Fig. 3. Luminosity-weighted mean age and metallicity vs. total $V - I$ color for those galaxies with quoted colors in Poulain & Nieto (1994) and Prugniel & Heraudeau (1998). The solid line in the bottom panel represents the transformation of the age-color and age-metallicity fits to the data to the metallicity-color plane.

3.3. Emission line measurements

Five galaxies have emission in at least two of the Hβ, [O III] [N II] or Hα lines (see Table 3). In two cases, NGC 1581 and NGC 3156, this emission is spatially resolved. According to the line-strength diagnostics of Kewley et al. (2001), NGC 2902 and NGC 1553 have unambiguous AGN emission. We are unable to distinguish between thermal and non-thermal emission for the other galaxies, though in those with spatially-resolved emission some contribution must come from star-formation. NGC 1581 also has strong (thermal) emission at $\sim$1 $\times$ $r_{\rm e}$ from the nucleus suggestive of a "ring" of on-going star formation.

4. Discussion

4.1. Galaxy color versus age and metallicity

Aragón-Salamanca et al. (2006) found the relationship between color and S_N for S0s is consistent with a fading stellar population. However, because of the age-metallicity degeneracy, they were unable to confirm that this was truly an age effect. Now that we have separated age and [Fe/H], we can tackle this question directly. Figure 3 shows $V - I$ color versus age and metallicity. This plot clearly indicates that age is strongly correlated with $V - I$ while metallicity is less so. A Spearman rank-correlation test indicates that the $V - I$ log Age correlation is significant at greater than the 99% level, while that of metallicity is <94%. The variation of [Fe/H] with color can be explained by the age-color relationship and the age-metallicity degeneracy. On the bottom panel in Fig. 3 we plot the linear fits to the our age-color and age-metallicity data transformed to the metallicity-color plane. The residuals from this fit are not correlated with color. The galaxies plotted here are a subset of those in Aragón-Salamanca et al. (2006). We thus confirm that their result was correctly interpreted as an age effect rather than being due to metallicity.

4.2. The formation of S0 galaxies

Figure 4 shows the derived ages versus globular cluster specific frequency. Also shown is the relationship expected from population synthesis models of a fading stellar population

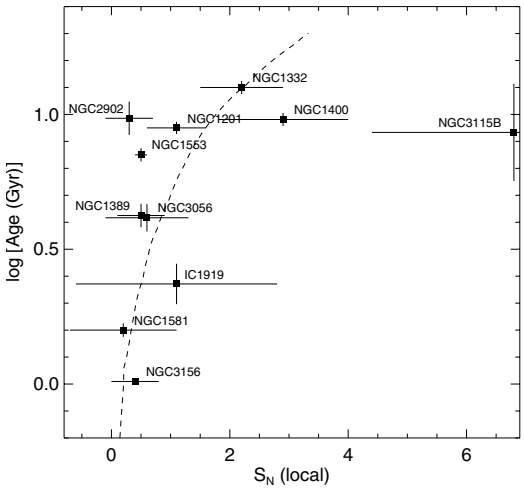

Fig. 4. Log age in Gyr vs. globular cluster specific frequency (S_N) for our sample. The line shows the evolution expected for a fading galaxy which starts out with $S_N = 0.4$ according to the stellar population models of Bruzual & Charlot (2003).

(Bruzual & Charlot 2003). This relationship is normalised to a spiral with $S_N = 0.4$. We note that younger S0s are found with S_N close to the spiral values whereas older S0s are nearer the average elliptical S_N.

Our results are consistent with those presented in Aragón-Salamanca et al. (2006) and support the theory that S0 galaxies evolve from fading spirals. It is important to understand that the distribution of our points on the Age-S_N diagram is not an evolutionary sequence with galaxies moving from one point to another. Rather S0s will evolve differently according to their mass and the total number of globular clusters. However, the galaxies do occupy the locus of points expected from the fading population model and occupy that space between the average spiral S_N and average elliptical S_N.

The fact that there are no young galaxies with large values of S_N indicates that large numbers of globular clusters are not created when S0s form. More precisely, any increase in the number of globular clusters must be accompanied by an increase of the same factor in the luminosity of the galaxy to stop S_N increasing.

4.3. Correlations between M_V, age, [α/Fe], and σ

A number of relationships are expected, and indeed found, for our sample of galaxies. Before drawing any conclusions we need to establish firmly that these do not affect our Age$-S_N$ plot in a way that might mimic the effect of a fading stellar population. The strongest correlations seen in our data are (1) the Faber-Jackson relation ($M_V - \sigma$), (2) M_V- [α/Fe], and (3) M_V-log Age. The first two relationships are well established (e.g. Faber & Jackson 1976; Jørgensen 1999; Trager et al. 2000), and the latter two are a manifestation of the "downsizing" phenomenon. Qualitatively this says that massive galaxies are older and formed more quickly (see e.g. Cowie et al. 1996; Gavazzi et al. 1996; Boselli et al. 2001). Relationship (3) will have the most direct effect on our Age $-S_N$ plot as M_V enters the definition of S_N directly. For the galaxies in our sample $\log \text{Age} = -0.326 M_V - 5.73$.

The M_V-log Age relation cannot mimic the fading of a stellar population on the Age $-S_N$ diagram. In the former case, older galaxies are brighter and so will tend to have lower S_N. In a fading population the opposite is true. The reality will be slightly more complex as brighter galaxies tend to have more clusters. However, it is clear that the M_V-log Age relationship acts in a different direction and so cannot be responsible for our Age $-S_N$ distribution.

4.4. On-going star formation

It has been suggested that an environment-induced transformation from spiral to S0 may be accompanied by a starburst (e.g. Milvang-Jensen et al. 2003; Dressler et al. 2004; Bamford et al. 2005). The two youngest galaxies in our sample do indeed show signs of on-going star-formation. The rest of the galaxies have luminosity-weighted mean ages greater than 2 Gyr. This is probably longer than any environment-induced burst would last and so we would not reasonably expect to see forming stars in these galaxies. The pertinent question is whether the star-formation in the youngest galaxies can be traced to a burst $\sim$1 Gyr in the past, or represents the last vestiges of normal spiral activity. The duration of a starburst can be expected to be of order a group-or-cluster crossing time ($\lesssim 10^8$ yr), and we predict that it will use up the galactic gas reservoir more quickly than normal star formation. It therefore seems more likely that current emission lines represent the dying embers of regular spiral activity. The fact of on-going star-formation also argues against a rapid method of creation for lenticulars. It is difficult to envision star formation lasting $\simeq$1 Gyr for any scenario involving close galaxy interactions or mergers. However, a complete rejection of a violent formation scenario using this argument is premature given that we are speculating on the nature of line emission in just two galaxies.

4.5. Comparison with other studies

A number of methods of transforming spirals to lenticulars have been proposed (see Sect. 1). As mentioned before, however, observational studies, rather than plausible simulations are less numerous. Studies of rich clusters at intermediate redshift show that S0s must have undergone starbursts in the not too distant past (e.g. Treu et al. 2003; Dressler et al. 2004; McIntosh et al. 2004; Barr et al. 2006). Other studies favouring the "violent" formation scenario show tidally-induced star formation (e.g. Boselli et al 2005) or ram-pressure-induced star formation (e.g. Sun et al. 2006).

A gentler transformation from spiral to S0 is implied by the studies of Bedregal et al. (2006) and Boselli et al. (2006). Our observations are consistent with fading of the stellar populations. This, combined with the on-going star formation in our youngest galaxies leads the present study toward the gentler formation mechanism. It must be borne in mind, however, that our galaxies generally reside in poorer environments than those supporting the more rapid transformation mechanisms. This may signal an important distinction with starbursts more common in richer environments and a study of the differences between cluster, group and field S0s would address this issue. For the moment, our sample does not allow us to draw conclusions in this area.

4.6. NGC 3115B

If our understanding of the evolution in the Age, S_N plane is correct then NGC 3115B shouldn't end up where it is. Kundu & Whitmore (2001b) note that this is a "cluster rich" dwarf galaxy and perhaps some of its larger neighbour's systems have been mistakenly assigned to it. This would suggest that S_N should be

lower than quoted. It is an outlier by over 3 mag on the $M_V - S_N$ relation.

5. Summary

We test the theory that S0 galaxies formed from spirals whose star formation is shut off and who evolve passively from that moment. Using EMMI on the NTT we have taken long slit spectroscopy of eleven lenticular (S0) galaxies at $z < 0.006$. We derive absorption line indices from the central $r_e/8$ of each galaxy. These measurements are then used, together with stellar population models to estimate relative ages, metallicities and α-element abundance ratios.

The derived physical properties are compared with globular cluster specific frequency (S_N). We find that S_N is correlated with age. The values of S_N span the range of average values for spirals to the average value of ellipticals. Our galaxies occupy the locus of points on the Age$-S_N$ diagram expected for a stellar population fading from the average spiral S_N. We confirm that previous results showing a relationship between S_N and color are driven by the S_N-Age effect.

Our results are consistent with the hypothesis that S0 galaxies are formed from spirals. An individual galaxy's position on the Age$-S_N$ plot is a function of the time since the cessation of star formation. The two youngest galaxies in our sample have extended emission lines indicating on-going star-formation. This points to a timescale over which star formation is shut down which is of order 1 Gyr. We speculate that the truncation of star formation may therefore be a gentle process involving few, if any, major bursts.

Acknowledgements. We thank the referee, Alessandro Boselli, for insightful comments which improved this paper. M.R.M. is supported by a PPARC Senior Fellowship. Based on observations made with the NTT ESO telescope at La Silla observatory under programme ID 076.B-0182(A)

References

Aragón-Salamanca, A., Bedregal, A. G., & Merrifield, M. R. 2006, A&A, 458, 101
Ashman, K. M., & Zepf, S. E. 1998, Globular cluster systems (Cambridge, UK, New York: Cambridge University Press, Cambridge astrophysics series; 30)
Bamford, S. P., Milvang-Jensen, B., Aragón-Salamanca, A., & Simard, L. 2005, MNRAS, 361, 109
Barr, J. M., Jørgensen, I., Chiboucas, K., Davies, R. L., & Bergmann, M. 2006, ApJ, 649, L1
Bedregal, A. G., Aragón-Salamanca, A., & Merrifield, M. R., 2006, MNRAS, 373, 1125
Bekki, K. 1998, ApJ, 502, 133
Boselli, A., Gavazzi, G., Donas, J., & Scodeggio, M. 2001, AJ, 121, 753
Boselli, A., Boissier, S., Cortese, L., et al. 2005, ApJ, 623, L13
Boselli, A, Bossier, S., Cortese, L., Gil de Paz, A., Siebert, M., Madore, B. F., Buat, V., Martin, D. C. 2006, ApJ, 651, 811
Bruzual, G., & Charlot, S. 2003, MNRAS, 344, 1000
Cappellari, M., & Emsellem, E. 2004, PASP, 116, 138
Corwin, H., G., Jr., Buta, R. J., & de Vaucouleurs G. 1994, AJ, 108, 2128
Cowie, L. L., & Songaila, A. 1977, Nature, 266, 501
Cowie, L. L., Songaila, A., Hu, E. M., & Cohen, J. G. 1996, AJ, 112, 839
Davies, R. L., Sadler, E. M., & Peletier, R. F. 1993, MNRAS, 262, 650
Dekker, H., Delabre, B., & Dodorico, S. 1986, Proc. SPIE, 627, 339
Dressler, A., Oemler, A., Couch, W., et al. 1997, ApJ, 490, 577
Dressler, A., Oemler, A. J., Poggianti, B. M., et al. 2004, ApJ, 617, 867
Faber, S. M., & Jackson, R. E. 1976, ApJ, 204, 668
Flores, H., Hammer, F., Puech, M., Amram, P., & Balkowski, C. 2006, A&A, 455, 107
Gavazzi, G., Pierini, D., & Boselli, A. 1996, A&A, 312, 397
Gebhardt, K., Richstone, D., Kormendy, J., et al. 2000, AJ, 119, 1157
Gnedin, O. Y. 2003a, ApJ, 582, 141
Gnedin, O. Y. 2003b, ApJ, 589, 752
Goudfrooij, P., Strader, J., Brenneman, L., et al. 2003, MNRAS, 343, 665
Gunn, J. E., & Gott, J. R. I. 1972, ApJ, 176, 1
Harris, W. E., & van den Bergh, S. 1981, AJ, 86, 1627
Jørgensen, I. 1997, MNRAS, 288, 161
Jørgensen, I. 1999, MNRAS, 306, 607
Kewley, L. J., Dopita, M. A., Sutherland, R. S., Heisler, C. A., & Trevena, J. 2001, ApJ, 556, 121
Kundu, A., & Whitmore, B. C. 2001, AJ, 121, 2950
Kundu, A., & Whitmore, B. C. 2001, AJ, 122, 1251
Kuntschner H., Ziegler B., Sharples R. M., Worthey G., & Fricke K. J., 2002, A&A, 395, 761
Larson, R. B., Tinsley, B. M., & Caldwell, C. N. 1980, ApJ, 237, 692
McIntosh, D. H., Rix, H.-W., & Caldwell, N. 2004, ApJ, 610, 161
Mihos, J. C., & Hernquist, L. 1994, ApJ, 425, L13
Milvang-Jensen, B., Aragón-Salamanca, A., Hau, G. K. T., Jørgensen, I., & Hjorth, J. 2003, MNRAS, 339, L1
Moore, B., Katz, N., Lake, G., Dressler, A., & Oemler, A. 1996, Nature, 379, 613
Moore, B., Lake, G., & Katz, N. 1998, ApJ, 495, 139
Poggianti B., Bridges, T. J., Mobasher, B., et al. 2001, ApJ, 562, 689
Poulain, P., & Nieto, J.-L. 1994, A&AS, 103, 573
Prugniel, P., & Heraudeau, P. 1998, A&AS, 128, 299
Quilis, V., Moore, B., Bower, R. 2000, Science, 288, 1617
Sakai, S., Mould, J. R., Hughes, S. M. G., et al. 2000, ApJ, 529, 698
Sun, M., Jones, C., Forman, W., et al. 2006, ApJ, 637, L81
Terlevich A. I., Kuntschner H., Bower R. G., Caldwell N., & Sharples R. M., 1999, MNRAS, 310, 445
Thomas, D., Maraston, C., & Bender, R. 2003, MNRAS, 339, 897
Thomas, D., Maraston, C., Korn, A. 2004, MNRAS, 351, L19
Thomas, D., Maraston, C., Bender, R., & Mendes de Oliveira, C. 2005, ApJ, 621, 673
Trager, S. C., Faber, S. M., Worthey, G., & González, J. J. 2000, AJ, 120, 165
Treu, T., Ellis, R. S., Kneib, J.-P., et al. 2003, ApJ, 591, 53
Vollmer, B., Cayatte, V., Balkowski, C., & Duschl, W. J. 2001, ApJ, 561, 708
Weiner, B. J., Willmer, C. N. A., Faber, S. M., et al. 2006, ApJ, 653, 1049
Worthey, G. 1994, ApJS, 94, 107
Worthey, G., & Ottavani, D. L. 1997, ApJS, 111, 377